Accepted Manuscript

Correlation of HPPMS plasma and coating properties using artificial neural networks

K. Bobzin, T. Brögelmann, N.C. Kruppe, M. Arghavani, M. Engels

PII: S0257-8972(18)30641-8
DOI: doi:10.1016/j.surfcoat.2018.06.065
Reference: SCT 23517

To appear in: *Surface & Coatings Technology*

Received date: 1 March 2018
Accepted date: 25 June 2018

Please cite this article as: K. Bobzin, T. Brögelmann, N.C. Kruppe, M. Arghavani, M. Engels , Correlation of HPPMS plasma and coating properties using artificial neural networks. Sct (2018), doi:10.1016/j.surfcoat.2018.06.065

Manuscript Cover Page (Surface and Coatings Technology)

Correlation of HPPMS Plasma and Coating Properties using Artificial Neural Networks

K. Bobzin, T. Brögelmann, N.C. Kruppe, M. Arghavani, M. Engels*

Surface Engineering Institute, RWTH Aachen University, Kackertstr. 15, 52072 Aachen, Germany

* Corresponding author.

Phone: +49 (0) 241 809-9368,

Fax number: +49 (0) 241 809-2941,

E-mail: engels@iot.rwth-aachen.de

Abstract

The development of industrial coating processes for tool coatings by means of physical vapor deposition (PVD) is usually extremely complex. This is caused by the large number of necessary coating batches and associated coating analyses until suitable process parameters are found. Artificial neural networks (ANN) are basically capable of describing complex relationships between various characteristic process values. Hence, within the scope of this paper the capability of describing complex correlations was tested on the example of a reactive high power pulsed magnetron sputtering (HPPMS) (Cr,Al)ON process. Selected process parameters pulse frequency and process gas composition were chosen, since they exhibit strongly non-linear cause-effect relationships. The ANN was used in order to correlate selective results from efficient substrate-oriented plasma diagnostics and coating analyses. Regarding the plasma properties the Al/Cr ratio and the metal-to-gas ion flux ratio were considered. With respect to the coating properties the Al/Cr ratio and the universal hardness were examined. From the correlation of these results, conclusions on the process parameters for desired coating properties were deduced and successfully proven for the investigated HPPMS (Cr,Al)ON process. Hence, the ANN exhibits a great potential to supplement the fundamental understanding of PVD processes in order to contribute to a simplification of the development of industrial coating processes.

Keywords:

Physical Vapor Deposition (PVD); High Power Pulsed Magnetron Sputtering (HPPMS/HiPIMS); Industrial Coating Process Development; Substrate-oriented Plasma Diagnostics; Hard Coatings (Cr,Al)ON; Artificial Neural Networks (ANN)

1 Introduction

The development of an industrial coating process using high power pulsed magnetron sputtering (HPPMS) to produce tool coatings with outstanding properties is usually extremely complex. This is caused by the numerous degrees of freedom for the process design and coating development, which result from the various process parameters. The coating formation is for example significantly influenced by the HPPMS pulse parameters pulse-on-time t_{on} and frequency f or the process gas pressure and its composition [1-7]. Further parameters which influence the coating properties are the bias voltage, the average cathode power, the substrate orientation and rotation as well as the heating. Hence, the coating development is either based on experience knowledge or rather on a significant effort in necessary coating batches until suitable process parameters are found. Furthermore, associated coating analyses have to be conducted in order to identify the desired coating properties for the addressed application.

In order to overcome this issue, a suitable approach is possible by using efficient plasma diagnostics. Plasma diagnostics enable a much faster analysis of process parameter variations, which results in a fundamental understanding of the cause-effect relationships between the process parameters and the plasma properties [8]. Hence, the HPPMS plasma has been subject to various plasma diagnostic experiments. An extensive overview on these results can be found in the work of Britun et al. [9] and especially for reactive HPPMS processes in the work of Anders [10]. In the next step it is possible to correlate the plasma properties with the coating properties. For example, it has been shown that the chemical composition of the plasma and the coating or the plasma ionization and the mechanical properties of the coating can be correlated [11]. Nevertheless, often strongly non-linear relations between the process parameters and the plasma and coating properties, respectively, are found which significantly complicate the correlation. Especially in order to analyze and describe these non-linear relations, the training of artificial neural networks (ANN) has been introduced in process and coating development for various applications like the prediction of (Ti,Al)N coating properties from dcMS process parameters [12] or tribological properties from coating properties [13]. These investigations exhibit a great potential regarding the simplified description of non-linear cause-effect relationships. Hence, applicability for the correlation of HPPMS plasma and coating properties can be assumed.

Therefore, this work provides a contribution to the usability of ANN regarding the correlation of HPPMS plasma and coating properties in order to simplify industrial coating development. The HPPMS is a frequently used technology, which is known as a technological advancement of the direct current (dc) and middle frequency (mf) magnetron sputtering (MS) [14-16]. Compared to these process variants, the HPPMS provides a significantly increased ionization of the metal and gas species [17-21], which also influence the corresponding coating properties [2-5]. For example, higher values of the mechanical properties have been observed, which correlate with a denser morphology, more homogeneous microstructure and a change of the chemical composition of the coating [6,7].

For the conducted experiments, the oxynitride coating system (Cr,Al)ON was chosen. The high interest regarding this coating system is based on its chemical and mechanical properties and hence the suitability for various applications, for example the coating of plastics processing tools [22]. Exemplarily for the large set of possible parameter variations, the process parameters pulse frequency f and the reactive gas flow ratio $j(O_2)/j(N_2)$ were chosen. Based on the results of substrate-oriented plasma diagnostics by means of optical emission spectroscopy (OES) and energy-resolved mass spectroscopy (ERMS) as well as coating analysis using scanning electron microscopy (SEM), glow discharge optical emission spectroscopy (GDOES) and nanoindentation, correlations of the process parameters with the plasma and coating properties were identified. Using the generated data, an artificial neural network (ANN) was trained, which connects the plasma and coating properties. The methodology for the simplification of an industrial coating development was finally validated with a coating experiment.

2 Experimental details

2.1 Coating unit configuration

The HPPMS plasma diagnostics and the coating deposition were conducted in an industrial scale PVD coating unit, CC800/9 Custom, CemeCon AG, Würselen, Germany, which has a vacuum chamber dimension of 1,000 mm x 1,000 mm x 1,000 mm (Fig. 1). A cathode with a HPPMS power supply was used. A Cr target with a purity of 99.9 % and 20 embedded Al plugs with a purity 99.5 % (CrAl20) and a size of 500 mm x 88 mm was mounted to the cathode.

2.2 Process parameters

The substrate-oriented plasma diagnostics and deposition of the (Cr,Al)ON coatings were conducted using a mean cathode power $P_{HPPMS} = 5.0$ kW with a constant pulse on time $t_{on} = 40$ µs. For the plasma diagnostics, the HPPMS frequency was varied in fixed steps $\Delta f = 100$ Hz from $f = 400$ Hz to $f = 1{,}000$ Hz and $\Delta f = 1{,}000$ Hz from $f = 1{,}000$ Hz to $f = 4{,}000$ Hz. The bias voltage was $U_B = 0$ V, since it could not be applied for the ERMS. For the coating deposition, frequencies $f = 500$ Hz, $f = 1{,}000$ Hz and $f = 2{,}000$ Hz were used. The bias voltage was $U_B = -100$ V. Ar was used as process gas. The Ar flow was j(Ar) = 200 sccm. N_2 and O_2 were used as reactive gases. The N_2 flow was determined by the pressure control to achieve p = 500 mPa with respect to the operating point of the HPPMS process. Three fixed O_2 flows $j(O_2) = 0.0$ sccm, $j(O_2) = 12.5$ sccm and $j(O_2) = 25.0$ sccm were investigated, which resulted in reactive gas flow ratios $j(O_2)/j(N_2) = 0.00$, $j(O_2)/j(N_2) = 0.23$ and $j(O_2)/j(N_2) = 0.50$. For all experiments the substrate table rotation was switched off in order to obtain comparable results. The substrate heating was switched off during the plasma diagnostics in order to prevent a damaging of the temperature sensitive in-situ equipment. For the coating deposition, the substrates were heated up to approx. $t_S = (350 \pm 20)$ °C.

2.3 Plasma diagnostics

The composition of the plasma regarding the composition of excited and ionized Al and Cr metal species was determined by means of optical emission spectroscopy (OES). An OES system EMICON HR, Plasus GmbH, Mering, Germany, was used. The intensity of the selected species was averaged from t_{OES} = 30 s measurement time. The collimator optics was mounted to a custom constructed holding unit. With this holding unit, the OES collimator optics was oriented parallel to the cathode surface at the substrate position. Hence, the distance between the line-of-sight of the collimator optics and the cathode was comparable to the distance of the substrates and was x = 60 mm (Fig. 1a).

The metal-to-gas ion flux ratio was determined by means of energy-resolved mass spectrometer (ERMS) Hiden EQP300, Hiden Analytical, Warrington, United Kingdom. The orifice of the ERMS had a diameter of d_{MaSp} = 150 µm. The ERMS was positioned at the substrate side using a flange in the wall opposite to the cathode, so that the orifice was in one axis perpendicular to the cathode as shown in Fig. 1b. The distance between the ERMS orifice and the HPPMS cathode also was x = 60 mm. It was electrically connected to the vacuum chamber wall and therefore grounded. A detailed description of the mass spectrometer can be found elsewhere [23, 24].

2.4 Coating characterization

The coatings were deposited on AISI 420 steel substrates (1.2083, X42Cr13, (54 ± 2) HRC, d_S = 22 mm) as shown in Fig 1c, conventionally used in plastics processing [25]. In order to evaluate the coating morphology, thickness and deposition rate, SEM Gemini, ZEISS DSM, Oberkochen, Germany, micrographs of fractured cross sections were taken using a secondary electrons (SE) detector. Additionally, micrographs of the surface morphology were recorded. The chemical composition of the coatings regarding the Al/Cr metal ratio was averaged from depth-resolved measurements by means of glow discharge optical emission spectroscopy (GDOES) JY 5000 RF, K.K. Horiba Seisakusho, Kyoto, Japan. The universal hardness HU was determined using nanoindentation. A TriboIndenter TI950, Bruker Corporation, Billerica, USA, was applied for this purpose. The indentation depth did not exceed 1/10 of the coating thickness to prevent substrate influence during the hardness measurement. The evaluation of the measured results was based on the equations according to Oliver and Pharr [26]. A constant Poisson's ratio of $\nu = 0.25$ was assumed. The value results from the average of c-CrN with $\nu = 0.28$ and h-AlN with $\nu = 0.22$ [22]. The measurements were conducted using a Berkovich indenter with a constant load for each indentation at 20 positions on the surface of the sample.

2.5 Artificial neural network

In order to identify the correlations between the measured plasma and coating properties, an artificial neural network (ANN) was trained. The software package MemBrain, Dipl.-Ing. Thomas Jetter, Mainz-Kostheim, Germany, was used for this purpose. A multilayer perceptron net with two different structures 1-5-5-1 and 1-5-5-5-1 was chosen, where the integer 1 defines the input and output parameters. The integer 5 is used for the description of the neurons in each hidden layer. For the training the ANN or rather the weighting of the synapses the resilient backpropagation algorithm was chosen. Approximately 500 training cycles were conducted for each correlation and net structure.

3 Results and Discussion

3.1 Evaluation of the plasma parameters

In the first step of the conducted experiments, the HPPMS (Cr,Al)ON plasma was analyzed by means of plasma diagnostics OES and ERMS. The HPPMS frequency was varied in the range from $f = 400$ Hz to $f = 4{,}000$ Hz, which was the accessible and technical relevant frequency range for the chosen process parameters. Furthermore, the reactive gas flow ratio was varied from $j(O_2)/j(N_2) = 0.00$ to $j(O_2)/j(N_2) = 0.50$. The other parameters were kept constant as described in section 2.2. The results of the OES measurements regarding the relative Al/Cr intensity ratio I_{Al}/I_{Cr} in the plasma are presented in Fig. 2. I_{Al}/I_{Cr} was determined from the excited and ionized metal species Al I, Al II, Cr I and Cr II.

As expected, strongly non-linear correlations between the process parameters and the plasma properties are observed. Generally, a decreasing trend can be found for I_{Al}/I_{Cr} when increasing the frequency f. Referring to the work of Greczynski et al., this behavior can be explained by the increased sputtering efficiency of Al, compared to Cr, when using HPPMS processes with higher power per pulse [27]. Furthermore, the values of I_{Al}/I_{Cr} increase for higher O_2 contents in the reactive gas, which might result from a higher target poisoning tendency for Cr, compared to Al, when adding O_2 to the reactive gas flow. Another aspect which must be taken into consideration can be found for frequencies between approx. f = 700 Hz and f = 1,000 Hz, especially for $j(O_2)/j(N_2) = 0.50$. For these frequencies the dependency of I_{Al}/I_{Cr} is changing significantly. This can only be explained with a higher sputtering efficiency of Al, compared to Cr, for these frequencies. Since Cr is generally higher ionized than Al, an interpretation could be a stronger back-attraction of Cr ions towards the target at these selected frequencies.

The corresponding results of the ERMS measurements regarding the relative metal-to-gas ion flux ratio J_M/J_G in the plasma are presented in Fig. 3. J_M/J_G was determined from ion energy distribution function (IEDF) of the once and twice ionized metal species Al^+, Al^{++}, Cr^+ and Cr^{++}. The process parameters were identical to the OES measurements.

The ERMS results regarding J_M/J_G also exhibit the expected strongly non-linear dependency with respect to the frequency f as well as the reactive gas flow ratio $j(O_2)/j(N_2)$. J_M/J_G increases for higher frequencies up to f = 800 Hz for $j(O_2)/j(N_2) = 0.00$, f = 700 Hz for $j(O_2)/j(N_2) = 0.23$ and f = 600 Hz for $j(O_2)/j(N_2) = 0.50$. For further increasing frequencies J_M/J_G decreases before a contrary behavior is observable at higher frequencies f > 1,000 Hz, whereas the trend is changing to lower frequencies and power per pulse for higher oxygen contents in the reactive gas flow. A comparable behavior was found in our previous work [28] for a (Cr,Al)N process. The low values of J_M/J_G at low frequencies can be explained by reduced sputtering due to the low duty cycle, where a strong background gas rarefaction and reduced sputter yields appear.

The peak of J_M/J_G is reached for a condition where the sputter yield and the metal ionization exhibit the highest values. At higher frequencies, the lower power per pulse results in a gas dominated dc-like plasma [28]. The shift of the dependency can be explained with the increasing target poisoning and hence decreasing metal ion content in the plasma, which is known to appear when adding O_2 to the reactive gas flow [29]. The same explanation can be applied to the generally lower values of J_M/J_G for higher O_2 contents in the reactive gas flow. Nevertheless, this explanation cannot be applied to the increasing values of J_M/J_G for the (Cr,Al)ON processes for frequencies $f > 1{,}000$ Hz which is in contrast to the (Cr,Al)N process in [28]

Generally, from the OES and ERMS measurements it can be concluded that the strongly non-linear behavior of J_M/J_G significantly complicates the correlation of the plasma and coating properties. However, it is not possible to explain each observed phenomena fundamentally without more extensive plasma diagnostics. For an efficient process development, the fundamental investigations of the plasma must be supplemented with a simplified methodology. As described in the introduction, an ANN exhibits a high potential for this purpose, since it is capable to describe non-linear correlations.

3.2 Determination of the coating properties

In order to deduce the necessary data for the training of the ANN regarding the correlation of plasma and coating properties, (Cr,Al)ON coatings were deposited with selected process parameters as second step of the experiments. The HPPMS frequency was also varied with values $f = 500$ Hz, $f = 1{,}000$ Hz and $f = 2{,}000$ Hz. The reactive gas flow ratio variation was comparable to the plasma diagnostics with $j(O_2)/j(N_2) = 0.00$, $j(O_2)/j(N_2) = 0.23$ and $j(O_2)/j(N_2) = 0.50$. The investigations on the morphology by means of SEM are presented in Fig 4. The deposition rate for each process which was deduced from the SEM pictures is shown in Fig 5.

From the SEM micrographs of the fracture cross sections in Fig. 4 it can be observed that all deposited (Cr,Al)N and (Cr,Al)ON coatings exhibit a dense microstructure with a smooth surface topography. The deduced deposition rate in Fig. 5 shows increasing values from $R \approx 1.8$ μm/h to $R \approx 10.0$ μm/h. Due to the higher duty cycle, increasing values of R are found for higher frequencies, whereas the averaged highest deposition rate is found for $j(O_2)/j(N_2) = 0.23$. A striking result can be found for $j(O_2)/j(N_2) = 0.50$, where obviously a significant target poisoning appears for f = 500 Hz and f = 1,000 Hz due to the high amount of O_2 in the reactive gas flow. The target poisoning increases for lower frequencies, which was not expected. It is reported that the higher power per pulse at lower frequencies reduces the target poisoning in reactive processes [30].

In order to identify quantifiable correlations between the plasma and coating properties for the training of the ANN, the Al/Cr metal ratio in the deposited coatings was determined using GDOES. The corresponding results are presented in Fig. 6. Furthermore, the universal hardness of the coatings was measured by means of nanoindentation. The results are shown in Fig. 7.

As it was expected from the plasma diagnostics, strongly non-linear correlations between the process parameters and plasma properties can be found. For a reactive gas flow ratio $j(O_2)/j(N_2) = 0$ it can be observed that the Al/Cr ratio decreases with an increasing frequency. This behavior can be explained with the increased sputtering efficiency for Al, compared to Cr, when using HPPMS with higher peak power densities [27]. However, when adding O_2 to the process gas, this relation cannot be applied. No distinct correlation is observable. This means that the addition of O_2 into the reactive gas flow significantly complicates the coating development for (Cr,Al)ON coatings by means of HPPMS. The same evidence can be applied to the correlation between the frequency f as well as the reactive gas flow ratio $j(O_2)/j(N_2)$ and the universal hardness HU of the deposited coatings in Fig. 7. As it was observed for the Cr/Al metal ratio, the addition of O_2 to the reactive gas flow changes the relation, especially when changing to $j(O_2)/j(N_2) = 0.5$. Hence, a distinct implication cannot be deduced from these results.

Generally, it can be concluded that there is no significant correlation between the process parameters and coating properties, when varying the HPPMS frequency f and the reactive gas flow ratio $j(O_2)/j(N_2)$. This behavior is comparable to the plasma properties, where also strongly non-linear cause-effect relationships were identified.

3.3 ANN training and validation

As described in the previous sections 3.1 and 3.2 strongly non-linear cause-effect relationships between the process parameters and the plasma and coating properties, respectively, were identified for the investigated HPPMS (Cr,Al)ON process with the selected process parameters. Hence, a direct correlation between the plasma and coating properties can hardly be identified. In order to overcome this issue, an ANN was trained as described in section 2.5. The results of the plasma and coating properties with the same process parameters were used. In the first step of the ANN training, the correlation between the Al/Cr intensity ratio in the plasma I_{Al}/I_{Cr} and the Al/Cr ratio in the coating was considered, which has been identified as reasonable in our previous work [19]. The results are presented in Fig. 8a. In the second step, the correlation between the metal-to-gas ion flux ratio J_M/J_G and the universal hardness HU as representative value for the mechanical properties of the coating was considered. This correlation has been investigated before in [28]. These results are presented in Fig. 8b.

Generally, a strongly non-linear cause-effect relationship between both plasma and coating properties is observable as expected. Nevertheless, except one spike for each correlation, the data exhibit a comprehensible trend, which is similar to a peak function or rather a polynomial function of third to fourth degree. Regarding the training of the ANN it can be deduced that the chosen net structures reproduce the strongly non-linear correlation between the plasma and coating properties sufficiently. Slight differences between the two net structures are observable.

The 1-5-5-5-1 net structure exhibits an improved adaptability to the data points compared to the 1-5-5-1 net structure. This results from the higher number of possible calculation operations as well as a higher number of weightable synapses. Hence, this net structure delivers more sufficient results. Nevertheless, it can be concluded that the methodology of using an ANN for the correlation of plasma and coating is successfully proven.

However, despite the sucessful adaption of the ANN to the data points, the usability of the ANN for the simplification the HPPMS (Cr,Al)ON coating development has to be validated. For this purpose, one Al/Cr ratio in the coating and one universal hardness HU were chosen from the ANN fits in Fig. 8 to deposit a (Cr,Al)ON coating with these properties. As marked by the yellow circles, a coating exhibiting the values $x_{Al}/x_{Cr} = 0.32$ and HU = 32 GPa should be deposited. The correlating plasma properties were $I_{Al}/I_{Cr} = 0.30$ and $J_M/J_G = 0.35$ according to Fig. 8. These values were correlated with the frequency f and the reactive gas flow ratio $j(O_2)/j(N_2)$ as depicted in Fig. 9a for I_{Al}/I_{Cr} and in J_M/J_G Fig. 9b, which represent all data points from the plasma diagnostics in Fig. 2 and Fig. 3. In both figures, the process parameters range, which complies with the chosen plasma properties, is marked with a yellow line. From both figures the most suitable set of process parameters was averaged, which was f = 700 Hz and $j(O_2)/j(N_2) = 0.32$. The other process parameters were identical to the previous investigations.

For the HPPMS (Cr,Al)ON coating with these process parameters an Al/Cr ratio $x_{Al}/x_{Cr} \approx 0.24$ and an universal hardness HU ≈ 31 GPa is measured. This proves that the deduction of the process parameters from the correlation of plasma and coating properties with the ANN was successful for the selected process. Hence, the ANN exhibits the potential for a significant simplification of the coating development and concurrently an improved economic efficiency in terms of development time and effort for coating deposition and analysis.

4 Conclusions

This paper provides a contribution to the usability of ANN for the simplification of industrial coating process development by the example of a reactive HPPMS (Cr,Al)ON process. In order to validate the methodology, selected process parameters pulse frequency and process gas composition were varied. Strongly non-linear cause-effect relationships were identified and described for the selected substrate-oriented plasma diagnostics and coating analyses. Based on the process and results data, the ANN was trained for the selected relations between the Al/Cr ratio in the plasma I_{Al}/I_{Cr} and in the coating x_{Al}/x_{Cr} as well as between the metal-to-gas ion flux ratio J_M/J_G and the universal hardness. From this correlations, conclusions on the process parameters pulse frequency and reactive gas flow ratio for desired coating properties Al/Cr ratio and universal hardness were deduced and successfully proven for the investigated HPPMS (Cr,Al)ON process. Due to the successful validation of the methodology, experiments on further process parameters like the bias voltage and coating systems like (Ti,Al)N as well as further plasma and coating properties will be conducted. Generally, it can be concluded that ANN exhibit a great potential to supplement the fundamental understanding of PVD processes in order to simplify the development of industrial coating processes in terms of development time and effort for coating deposition and analysis.

5 Acknowledgement

The authors gratefully acknowledge the financial support of the German Research Foundation, Deutsche Forschungsgemeinschaft (DFG), within the transregional collaborative research center TRR87/2 (SFB-TR 87) subproject C6, A4 and A1.

List of references

[1] G. Greczynski, J. Jensen, J. Böhlmark, L. Hultman, Microstructure control of CrNx films during high power impulse magnetron sputtering, Surf. Coat. Technol. 205 (2010) 118-130.

[2] J. Alami, P.A.O. Persson, D. Music, J.T. Gudmundsson, J. Böhlmark, U. Helmersson, Ion-assisted physical vapor deposition for enhanced film properties on nonflat surfaces, J. Vac. Sci. Technol. A 23 (2) (2005) 278-280.

[3] K. Bobzin, N. Bagcivan, P. Immich, S. Bolz, R. Cremer, T. Leyendecker, Mechanical properties and oxidation behaviour of (Al,Cr)N and (Al,Cr,Si)N coatings for cutting tools deposited by HPPMS, Thin Solid Films 517 (3) (2008) 1251-1256.

[4] M. Lattemann, A.P. Ehiasarian, J. Bohlmark, P.A.O. Persson, U. Helmersson, Investigation of high power impulse magnetron sputtering pretreated interfaces for adhesion enhancement of hard coatings on steel, Surf. Coat.Technol. 200 (2006) 6495-6499.

[5] A.P. Ehiasarian, A. Vetushka, Y.A. Gonzalvo, G. Safran, L. Szekely, P.B. Barna, Influence of high power impulse magnetron sputtering plasma ionization on the microstructure of TiN thin films, J. Appl. Phys. 109 (2011) 104314.

[6] N. Bagcivan, K. Bobzin, G. Grundmeier, M. Wiesing, O. Ozcan, C. Kunze, R.H. Brugnara, Influence of HPPMS pulse length and inert gas mixture on the properties of (Cr, Al)N coatings, Thin Solid Films 549 (2013) 192–198.

[7] C. Kunze, R.H. Brugnara, N. Bagcivan, K. Bobzin, G. Grundmeier, Surface chemistry of PVD (Cr,Al)N coatings deposited by means of direct current and high power pulsed magnetron sputtering, Surf. Interface Anal. 45 (2013) 1884–1892.

[8] K. Bobzin, N. Bagcivan, S. Theiß, J. Trieschmann, R. H. Brugnara, S. Preissing, A. Hecimovic, Influence of Ar/Kr ratio and pulse parameters in a Cr-N high power pulse magnetron sputtering process on plasma and coating properties, JVST A 32 (2014) 021513.

[9] N. Britun, T. Minea, S. Konstantinidis, R. Snyders, Plasma diagnostics for understanding the plasma–surface interaction in HiPIMS discharges: a review, J. Phys. D: Appl. Phys. 47 (2014) 224001.

[10] A. Anders, Tutorial: Reactive high power impulse magnetron sputtering (R-HiPIMS), J. Appl. Phys. 121 (2017) 171101.

[11] K. Bobzin, T. Brögelmann, N.C. Kruppe, M. Engels, Influence of dcMS and HPPMS in a dcMS/HPPMS Hybrid Process on Plasma and Coating Properties, Thin Solid Films 620 (2016) 188-196.

[12] A. S. M. Jaya, A. S. H. Basari, S. Z. M. Hashim, H. Haron, M. R. Muhamad, M. N. A. Rahman, Application of anfis in predicting of tialn coatings hardness, Aust. J. Basic & Appl. Sci. 5 (2011) 1647-1657.

[13] E. Schulz, T. Breitsprecher, Y. Musayes, S. Tremmel, T. Hosenfeldt, S. Wartzack, H. Meerkamp, Advanced Ceramic Coatings and Materials for Extreme Environment II (2012).

[14] D. Lundin, K. Sarakinos, An introduction to thin film processing using high-power impulse magnetron sputtering, J. Mat. Res. 27 (2012) 780-792.

[15] K. Sarakinos, J. Alami, S. Konstantinidis, High power pulsed magnetron sputtering: A review on scientific and engineering state of the art, Surf. Coat. Technol. 204 (2010) 1661-1684.

[16] V. Kouznetsov, K. Macak, J. M. Schneider, U. Helmersson, I. Petrov, A novel pulsed magnetron sputter technique utilizing very high target power densities, Surf. Coat. Technol. 122 (1999) 290-293.

[17] A. Anders, A review comparing cathodic arcs and high power impulse magnetron sputtering (HiPIMS), Surf. Coat. Technol. 257 (2014) 308-325.

[18] J. Bohlmark, J. Alami, C. Christou, A. P. Ehiasarian, U. Helmersson, Ionization of sputtered metals in high power pulsed magnetron sputtering, JVST A 23 (2005) 18-22.

[19] G. Greczynski, J. Lu, M. P. Johansson, J. Jensen, I. Petrov, J. E. Greene, L. Hultman, Role of Ti^{n+} and Al^{n+} ion irradiation (n=1,2) during $Ti_{1-x}Al_xN$ alloy film growth in a hybrid HIPIMS/magnetron mode, Surf. Coat. Technol. 206 (2012) 4202-4211.

[20] E. Lewin, D. Loch, A. Montagne, A. P. Ehiasarian, J. Patscheider, Comparison of Al-Si-N nanocomposite coatings deposited by HIPIMS and DC magnetron sputtering, Surf. Coat. Technol. 232 (2013) 680-689.

[21] K. Macák, V. Kouznetsov, J. Schneider, U. Helmersson, Ionized sputter deposition using an extremely high plasma density pulsed magnetron discharge, J. Vac. Sci. Technol. A 18 (2000) 1533-1537.

[22] K. Bobzin, T. Brögelmann, R. H. Brugnara, M. Arghavani, T.-S. Yang, Y.-Y. Chang, S.-Y- Chang, Investigation on plastic behavior of HPPMS CrN, AlN and CrN/AlN-multilayer coatings using finite element simulation and nanoindentation, Surf. Coat. Technol. 284 (2015) 310-317.

[23] C.V. Budtz-Jorgensen, Studies of electrical plasma discharges, PhD Thesis, Aarhus University (2001).

[24] J. Benedikt, A. Hecimovic, D. Ellerweg, A. von Keudell, Quadrupole mass spectrometry of reactive plasmas, J. Phys. D: Appl. Phys. 45 (2012) 403001.

[25] K. Bobzin, T. Brögelmann, G. Grundmeier, T. de los Arcos, M. Wiesing, N.C. Kruppe, (Cr,Al)N/(Cr,Al)ON Oxy-nitride Coatings deposited by Hybrid dcMS/HPPMS for Plastics Processing Applications, Surf. Coat. Technol. 308 (2016) 394-403.

[26] W.C. Oliver, G.H. Pharr, An improved technique for determining hardness and elastic modulus using load and displacement sensing indentation experiments, J. Mater. Res. 7 (1992) 1564.

[27] G. Greczynski, L. Hultman, Peak amplitude of target current determines deposition rate loss during high power pulsed magnetron sputtering, ‘
Vacuum 124 (2016) 1-4.

[28] K. Bobzin, T. Brögelmann, N.C. Kruppe, M. Engels, A. von Keudell, A. Hecimovic, A. Ludwig, D. Grochla, L. Banko, Fundamental study of an industrial reactive HPPMS (Cr,Al)N process, J. Appl. Phys. 122 (2017) 015302.

[29] M.M. Waite, S. Ismat Shah, Target poisoning during reactive sputtering of silicon with oxygen and nitrogen, Mat. Sci. Eng. B 140 (2007) 64-68.

[30] T. Kubart, M. Aiempanakit, J. Andersson, T. Nyberg, S. Berg, U. Helmersson, Studies of hysteresis effect in reactive HiPIMS deposition of oxides, Surf. Coat. Technol. 205 (2011) 303-306.

List of figure captions

Fig. 1: Set up of the substrate-oriented plasma diagnostics by means OES (a) and ERMS (b) as well as positioning of the substrates within the coating chamber of the industrial scale PVD coating unit CC800/9 in the top view (c)

Fig. 2: Substrate-oriented Al/Cr intensity ratio I_{Al}/I_{Cr} by means of OES for the HPPMS (Cr,Al)ON process with varying frequency f and reactive gas flow ratio $j(O_2)/j(N_2)$

Fig. 3: Substrate-oriented metal-to-gas ion flux ratio J_M/J_G by means of ERMS for the HPPMS (Cr,Al)ON process with varying frequency f and reactive gas flow ratio $j(O_2)/j(N_2)$

Fig. 4: Morphology of the coatings by means of SEM micrographs of fracture cross section for the HPPMS (Cr,Al)ON process with varying frequency f and reactive gas flow ratio $j(O_2)/j(N_2)$

Fig. 5: Deposition rate for the HPPMS (Cr,Al)ON process with varying frequency f and reactive gas flow ratio $j(O_2)/j(N_2)$

Fig. 6: Al/Cr metal ratio x_{Al}/x_{Cr} by means of GDOES for the HPPMS (Cr,Al)ON process with varying frequency f and reactive gas flow ratio $j(O_2)/j(N_2)$

Fig. 7: Universal hardness HU by means of nanoindentation for the HPPMS (Cr,Al)ON process with varying frequency f and reactive gas flow ratio $j(O_2)/j(N_2)$

Fig. 8: Universal hardness HU by means of nanoindentation for the HPPMS (Cr,Al)ON process with varying frequency f and reactive gas flow ratio $j(O_2)/j(N_2)$

Fig. 9: Universal hardness HU by means of nanoindentation for the HPPMS (Cr,Al)ON process with varying frequency f and reactive gas flow ratio $j(O_2)/j(N_2)$

Tables

Table 1: Process parameters for the HPPMS plasma diagnostics and coating depostion

process parameter	unit	plasma diagnostics	coating deposition
pressure p	mPa	500	500
Ar flow j(Ar)	sccm	200	200
N_2 flow j(N_2)	sccm	50 – 70	50 – 70
O_2 flow j(O_2)	sccm	0 – 25	0 – 25
dc substrate bias U_B	V	0	-100
substrate table rotation speed v_S	rpm	---	---
HPPMS cathode power P_{HPPMS}	kW	5	5
pulse length HPPMS t_{on}	µs	40	40
pulse frequency HPPMS f	Hz	400 – 4,000	500 – 2,000
HPPMS duty cycle D_{HPPMS}	%	1.6 – 16.0	2.0 – 8.0
HPPMS peak power P_p	kW	50 – 500	100 – 400
substrate temperature T_S	°C	---	350 ± 20

Highlights

- Plasma diagnostics and coating analysis of HPPMS (Cr,Al)N and (Cr,Al)ON
- Strongly non-linear relation between process parameters, plasma and coating
- ANN capable of describing the correlation between plasma and coating properties
- Great potential of ANN to simplify the development of industrial coating processes

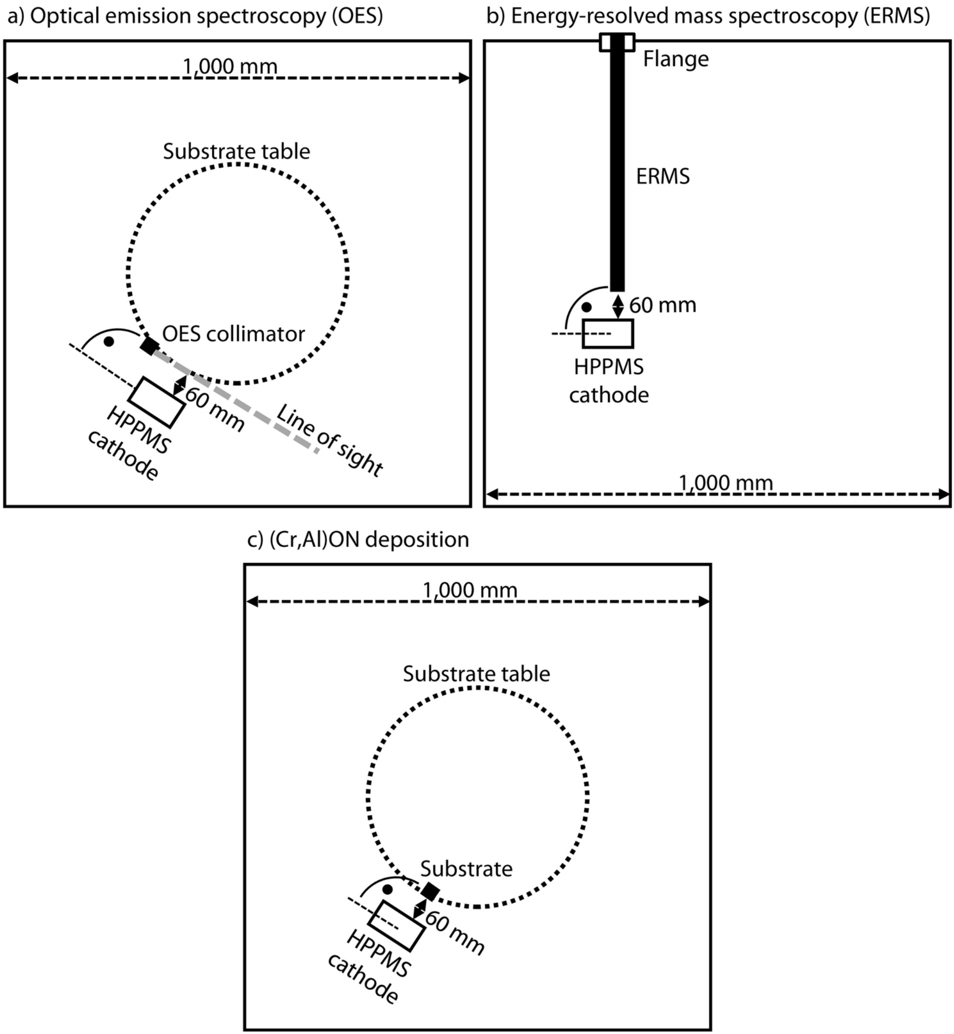

a) Optical emission spectroscopy (OES)
1,000 mm
Substrate table
OES collimator
60 mm
Line of sight
HPPMS
cathode
b) Energy-resolved mass spectroscopy (ERMS)
Flange
ERMS
60 mm
HPPMS
cathode
1,000 mm
c) (Cr,Al)ON deposition
1,000 mm
Substrate table
Substrate
60 mm
HPPMS
cathode

Figure 1

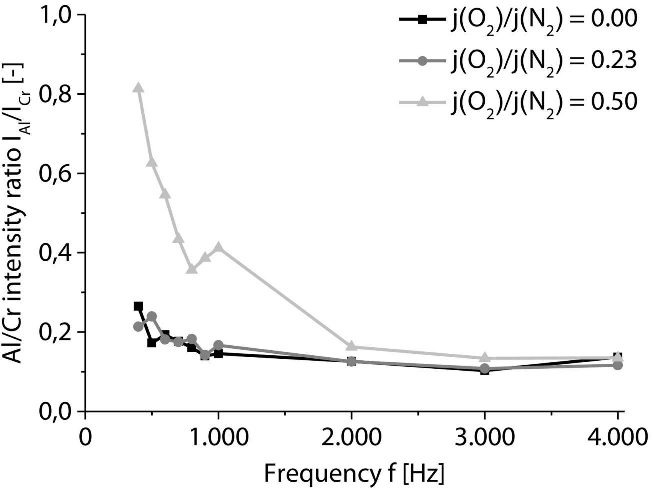

1,0
0,8
0,6
0,4
0,2
0,0
0
1.000
2.000
3.000
4.000
Al/Cr intensity ratio I_{Al}/I_{Cr} [-]
Frequency f [Hz]
$j(O_2)/j(N_2) = 0.00$
$j(O_2)/j(N_2) = 0.23$
$j(O_2)/j(N_2) = 0.50$

Figure 2

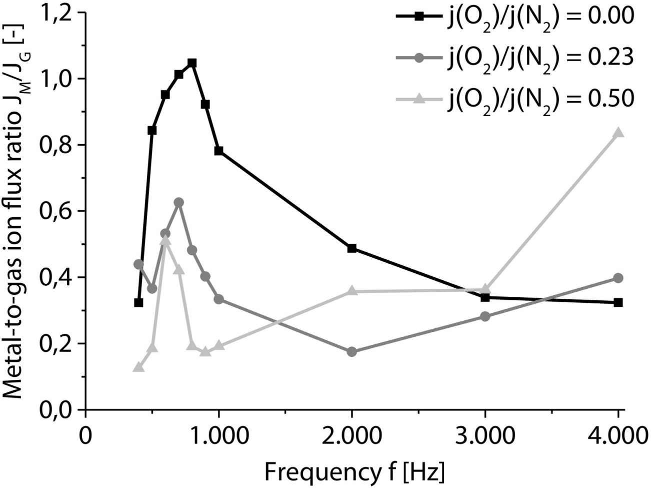

Metal-to-gas ion flux ratio J_M/J_G [-]
1,2
1,0
0,8
0,6
0,4
0,2
0,0
0
1.000
2.000
3.000
4.000
Frequency f [Hz]
$j(O_2)/j(N_2) = 0.00$
$j(O_2)/j(N_2) = 0.23$
$j(O_2)/j(N_2) = 0.50$

Figure 3

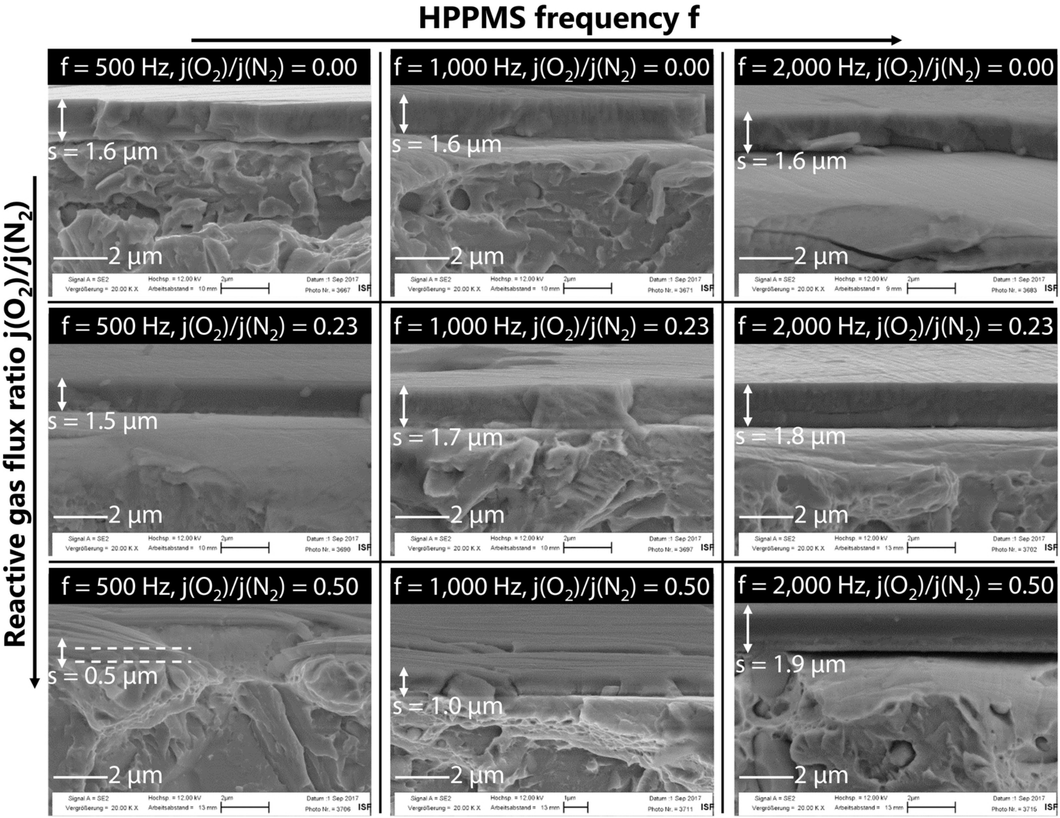
HPPMS frequency f
Reactive gas flux ratio j(O2)/j(N2)
f = 500 Hz, j(O2)/j(N2) = 0.00
s = 1.6 µm
2 µm
f = 1,000 Hz, j(O2)/j(N2) = 0.00
s = 1.6 µm
2 µm
f = 2,000 Hz, j(O2)/j(N2) = 0.00
s = 1.6 µm
2 µm
f = 500 Hz, j(O2)/j(N2) = 0.23
s = 1.5 µm
2 µm
f = 1,000 Hz, j(O2)/j(N2) = 0.23
s = 1.7 µm
2 µm
f = 2,000 Hz, j(O2)/j(N2) = 0.23
s = 1.8 µm
2 µm
f = 500 Hz, j(O2)/j(N2) = 0.50
s = 0.5 µm
2 µm
f = 1,000 Hz, j(O2)/j(N2) = 0.50
s = 1.0 µm
2 µm
f = 2,000 Hz, j(O2)/j(N2) = 0.50
s = 1.9 µm
2 µm

Figure 4

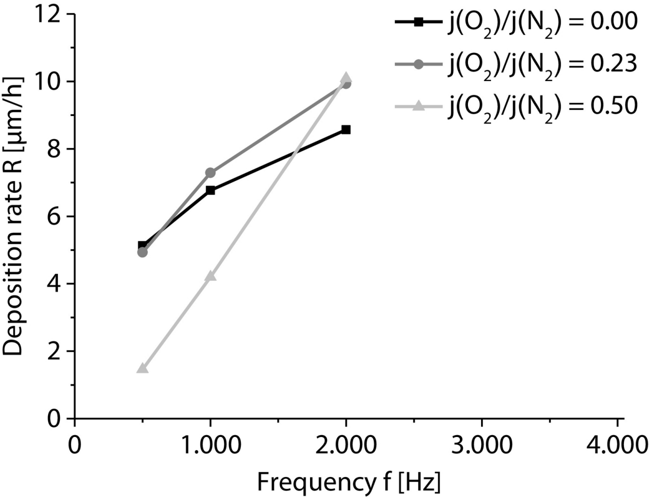

12
10
8
6
4
2
0
Deposition rate R [µm/h]
0
1.000
2.000
3.000
4.000
Frequency f [Hz]
$j(O_2)/j(N_2) = 0.00$
$j(O_2)/j(N_2) = 0.23$
$j(O_2)/j(N_2) = 0.50$

Figure 5

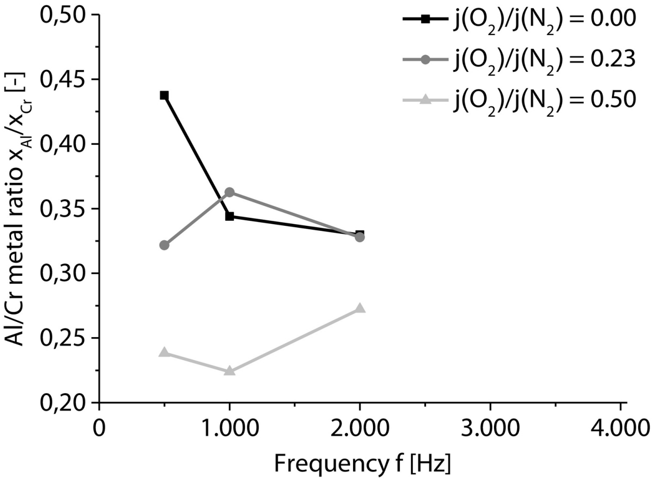

Al/Cr metal ratio x_{Al}/x_{Cr} [-]
0,50
0,45
0,40
0,35
0,30
0,25
0,20
0
1.000
2.000
3.000
4.000
Frequency f [Hz]
$j(O_2)/j(N_2) = 0.00$
$j(O_2)/j(N_2) = 0.23$
$j(O_2)/j(N_2) = 0.50$

Figure 6

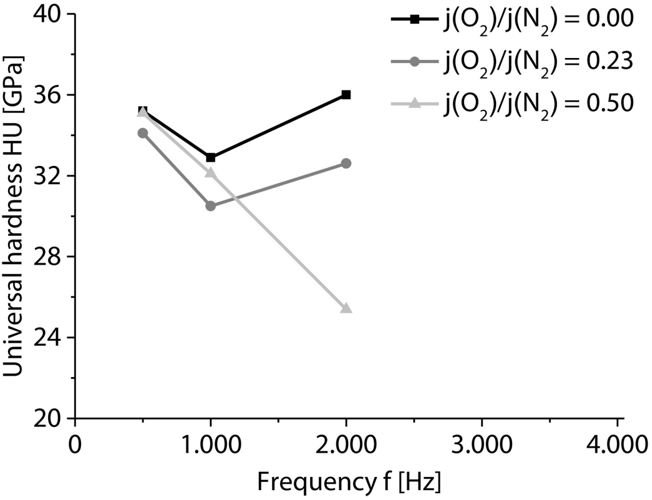

40
36
32
28
24
20
0
1.000
2.000
3.000
4.000
Universal hardness HU [GPa]
Frequency f [Hz]
j(O2)/j(N2) = 0.00
j(O2)/j(N2) = 0.23
j(O2)/j(N2) = 0.50

Figure 7

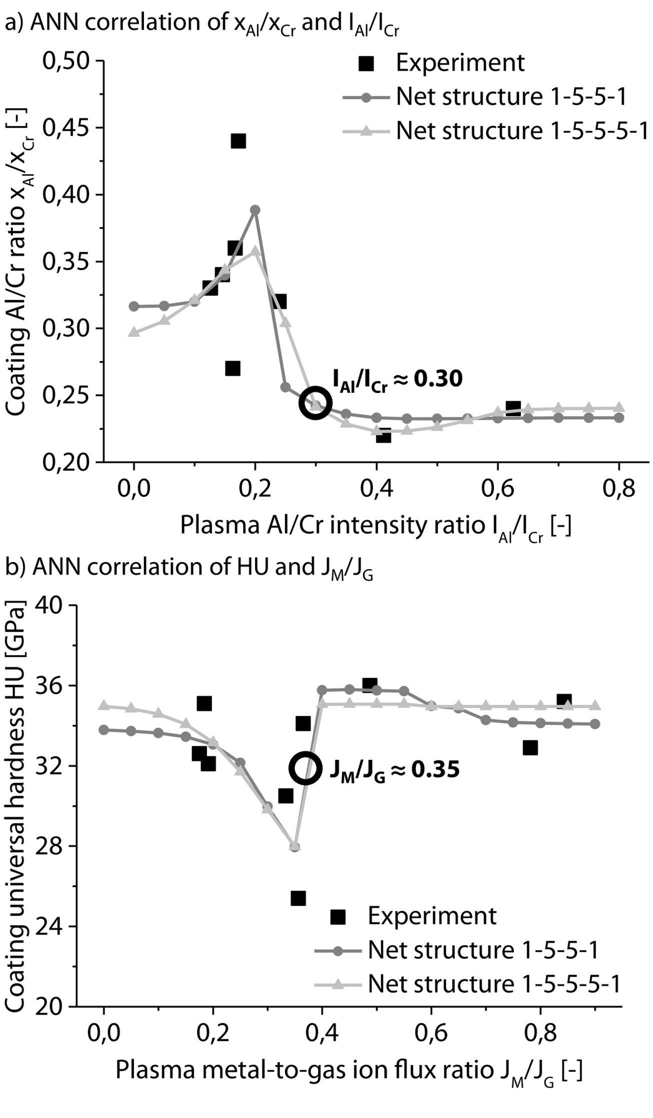

a) ANN correlation of x_Al/x_Cr and I_Al/I_Cr
Experiment
Net structure 1-5-5-1
Net structure 1-5-5-5-1
I_Al/I_Cr ≈ 0.30
Coating Al/Cr ratio x_Al/x_Cr [-]
Plasma Al/Cr intensity ratio I_Al/I_Cr [-]
0,50
0,45
0,40
0,35
0,30
0,25
0,20
0,0
0,2
0,4
0,6
0,8
b) ANN correlation of HU and J_M/J_G
J_M/J_G ≈ 0.35
Experiment
Net structure 1-5-5-1
Net structure 1-5-5-5-1
Coating universal hardness HU [GPa]
Plasma metal-to-gas ion flux ratio J_M/J_G [-]
40
36
32
28
24
20
0,0
0,2
0,4
0,6
0,8

Figure 8

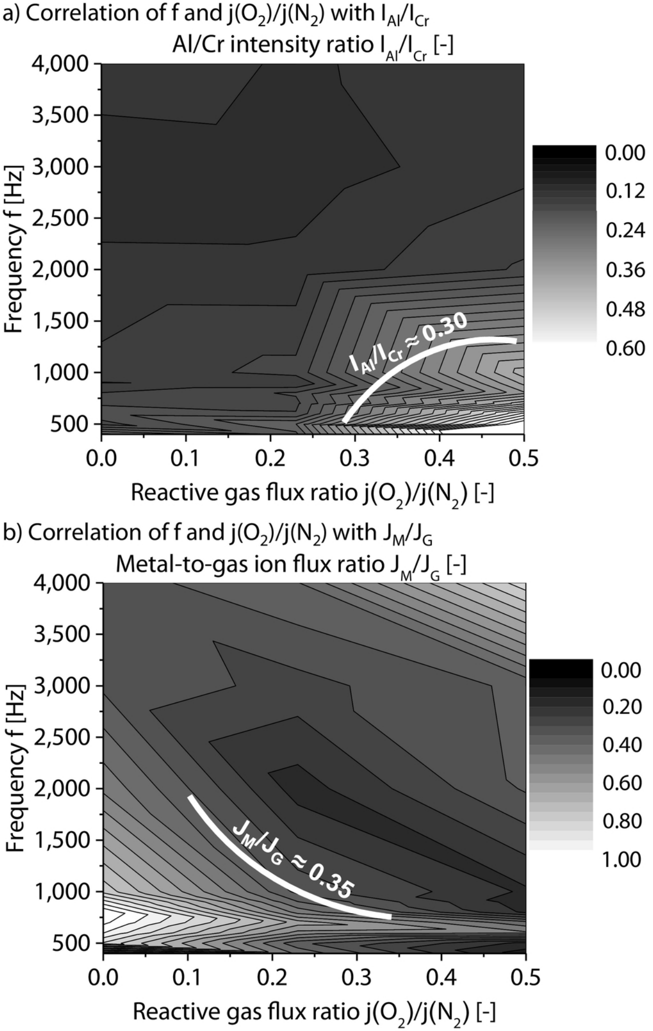

a) Correlation of f and j(O2)/j(N2) with IAl/ICr
Al/Cr intensity ratio IAl/ICr [-]
4,000
3,500
3,000
2,500
2,000
1,500
1,000
500
Frequency f [Hz]
0.00
0.12
0.24
0.36
0.48
0.60
IAl/ICr ≈ 0.30
0.0
0.1
0.2
0.3
0.4
0.5
Reactive gas flux ratio j(O2)/j(N2) [-]
b) Correlation of f and j(O2)/j(N2) with JM/JG
Metal-to-gas ion flux ratio JM/JG [-]
4,000
3,500
3,000
2,500
2,000
1,500
1,000
500
Frequency f [Hz]
0.00
0.20
0.40
0.60
0.80
1.00
JM/JG ≈ 0.35
0.0
0.1
0.2
0.3
0.4
0.5
Reactive gas flux ratio j(O2)/j(N2) [-]

Figure 9